INTERNATIONAL JOURNAL OF INTEGRATED ENGINEERING
ISSN: 2229-838X e-ISSN: 2600-7916

IJIE

Vol. 17 No.50 (2025) 77-86
https://publisher.uthm.edu.my/ojs/index.php/ijie

Flowability Properties of PLA/PA12 Composite with Varying Wollastonite Concentrations for 3D Printing Applications

Nur Munirah Mustaza[1], Farrahshaida Mohd Salleh[1]*, Abdul Manaf Abdullah[1], Mohd Ikram Ramli[2], Izdihar Tharazi[1], Muhammad Hussain Ismail[1]

[1] *Faculty of Mechanical Engineering, Universiti Teknologi MARA, 40450 Shah Alam, Selangor, MALAYSIA*
[2] *School of Engineering, University of Wollongong Malaysia, Glenmarie Campus, 40150 Shah Alam, Selangor, MALAYSIA*

*Corresponding Author: fshaida@uitm.edu.my
DOI: https://doi.org/10.30880/ijie.2025.17.05.007

Article Info

Received: 16 July 2024
Accepted: 22 June 2025
Available online: 30 August 2025

Keywords

Polylactic acid, polyamide 12, wollastonite, rheology, 3D printing

Abstract

This study evaluates the rheological properties and flow behaviour of PLA/PA12 composites with varying concentrations of wollastonite (WA) ceramic particles (5, 10, and 15 wt.%) to enhance their biological performance and printability in 3D printing applications. Achieving the right balance of viscosity and flow is crucial for producing high-quality filaments and reliable 3D printed structures. Comprehensive rheological analysis and material characterization were conducted, including particle size distribution, SEM, and EDX. The flow behaviour index (n) was calculated, and physical observations of extruded materials were assessed for surface quality and dimensional consistency. The 10 wt.% WA composite consistently demonstrated superior rheological properties, exhibiting optimal pseudoplastic behavior with an n value range of 0.073–0.439 and a viscosity of 5919 Pa·s at 140 °C, which was the lowest among the composites tested, ensuring smooth extrusion and structural integrity. SEM analysis showed a uniform microstructure with well-dispersed WA particles in the 10 wt.% WA composite, while the 5 wt.% WA and 15 wt.% WA composites displayed suboptimal particle distribution. Physical observations confirmed that the 10 wt.% WA composite produced a smooth, consistent extrudate, essential for high-quality filament fabrication and reliable 3D printing. These findings highlight the 10 wt.% WA composite as the most promising candidate for efficient and effective 3D printing.

1. Introduction

Three-dimensional (3D) printing has revolutionized manufacturing by offering a versatile, sustainable, and user-friendly method for creating complex parts. This technology has gained significant traction globally, with widespread adoption across various industries. Fused Deposition Modeling (FDM), a popular 3D printing process, has become a cornerstone of additive manufacturing. FDM uses a material extrusion method, where thermoplastic polymers are melted and extruded through a nozzle to build objects layer by layer. This process offers numerous advantages, including creating complex structures with high porosity at various scales, rapid prototyping, and

cost-effective production (1,2). The ease of use and flexibility of FDM has made it an attractive option for industrial and bone tissue engineering. FDM allows precise control over the spacing between deposited layers and manages interconnected internal structure thus creating uniform and complex scaffolds suitable for bone implants (3).

Rheology, the study of the flow and deformation of materials under applied forces or stresses, is crucial in understanding the 3D printing process. In 3D printing, rheological properties play a pivotal role in the deposition process, as they influence the material's ability to flow through the nozzle, adhere to previous layers, and maintain its shape during and after deposition (4). Rheological studies can assist in identifying and mitigating printing defects such as filament buckling, die swelling, and backflow. By understanding the viscoelastic behaviour of the material during the printing process, researchers can gain insights into the changes in viscosity and shear stress experienced by the material as it flows through different regions of the nozzle (5). This knowledge is crucial for optimizing printing parameters and material formulations. Furthermore, the non-Newtonian behaviour of the materials used in 3D printing is an important consideration. Shear-thinning behaviour, where the viscosity decreases with increasing shear rate, is desirable as it facilitates material flow during deposition while maintaining structural integrity after extrusion. Rheological studies can help identify and characterize this behaviour, enabling the development of materials tailored for optimal printing performance.

Polylactic acid (PLA), a biodegradable and biocompatible thermoplastic derived from renewable resources, is widely used in applications ranging from packaging to biomedical devices. Polyamide 12 (PA12), known for its excellent mechanical properties, chemical resistance, and low moisture absorption, enhances the performance of PLA when used in composites. Several studies have investigated the properties of PLA/PA12 composites using various processing methods and blend ratios. Raj et al. demonstrated that PA12 is the most compatible type of polyamide for blending with PLA through twin-screw extrusion without a compatibilizer, compared to PA10-10, PA10-12, and PA11. Their findings revealed that PLA/PA12 blends exhibited the highest melt-state compatibility, the lowest interfacial tension, and the closest surface tension values. Consequently, these blends showed significant improvements in tensile properties, achieving a brittle-to-ductile transition and a strain at break of approximately 170% for 40 wt% PA12 content compared to 10-30 wt.% of PA12 (6). Another study by Raj et al. investigated the role of poly(L-lactide) grafted maleic anhydride (PLA-g-MA) as a compatibilizer in 70/30 wt.% PLA/PA12 blends. The addition of PLA-g-MA (0 to 5 wt.%) significantly improved ductility, with the highest elongation at break of around 290% achieved with 1 wt.% PLA-g-MA (7). Murariu et al. tested various compositions of PLA/PA12 with 20-80% addition of PA12, identifying the 50/50 PLA/PA12 blend with 2% Joncryl compatibilizer as the most promising. This blend exhibited a tensile strength of 52 MPa, a strain at break of 175%, Young's modulus of 1930 MPa, and an impact resistance of 4.4 kJ/m^2, attributed to the compatibilizer's effect on co-continuous morphology and improved interactions between PLA and PA12 (8). These studies collectively demonstrate that incorporating PA12 and compatibilizers significantly enhances the mechanical of PLA, making these composites suitable for durable engineering applications. However, despite their improved mechanical properties, these blends are unsuitable for implant purposes due to potential acidic degradation and lack of biological activity. Therefore, in this study, wollastonite (WA), a bioceramic material, will be used to enhance the PLA/PA12 composite to improve the biological performance of the composite while maintaining its mechanical strength suitable for implant applications using FDM approach.

Wollastonite (WA) calcium silicate bioceramic material has gained significant attention recently due to its potential applications in biomedical implants. WA bioceramic exhibits excellent biocompatibility and bioactivity, which can promote osteointegration in composites, along with favorable mechanical properties, making it an attractive alternative to other bioceramic materials (9). WA can enhance the biological response through controlled ion release, supporting cell attachment and mineralization. Its silicate structure promotes apatite formation, which increases surface roughness and improves cellular response (10). Studies have shown that WA bioceramics can be successfully combined with PLA to create composite filaments suitable for FDM, providing enhanced biological activity and improved mechanical properties (3,9,11). The addition of WA to PLA enhances the mechanical and biological properties of the composite, making it an attractive option for biomedical applications. In addition, the high thermal stability of WA, which is up to 1000 °C, ensures no degradation during the extrusion and printing processes. The content of WA in the polymer matrix can significantly impact the final properties of the composite. For example, higher WA content can improve the biocompatibility of the composite but lower the mechanical strength due to the agglomeration of ceramic particles, while a lower content may enhance its flexibility and printability but lack biological activity. Further research is needed to optimize the composition of WA bioceramics composite filaments to ensure their suitability for various biomedical applications.

This study developed polymer-ceramic composites by incorporating varying concentrations (5, 10, and 15 wt.%) of WA into 80PLA/20PA12 composite using a melt-blending process. The composites were characterized using particle size distribution analysis, Scanning Electron Microscopy (SEM), and Energy-Dispersive X-ray Spectroscopy (EDX) to confirm the composition and analyze the morphological properties. Finally, rheological tests were conducted across a range of temperatures and shear rates to fulfill the aim of this study, which is to

Int. Journal of Integrated Engineering Vol. 17 No. 5 (2025) p. 77-86

determine the optimal content of WA particles in the PLA/PA12 composite that exhibits the best rheological properties for 3D printing applications.

2. Material and Methods

2.1 Raw Materials

The primary raw materials used in this study are medical-grade PLA coarse powder, PA12 powder and WA bioceramic, as illustrated in Fig. 1. The PLA, purchased from China (Grade PDLLA 40), has a 1.28 g/cm^3 density. The PA12, a binary polymer, is the HP 3D High Reusability grade. The WA was sourced from CNPC Powder Material Co., Ltd., China, with a 2.65 g/cm^3 density. Scanning Electron Microscopy (SEM) images of PLA and WA, shown in Fig. 2, reveal distinct morphologies: the PLA coarse powder consists of spherical particles with irregular shapes, while the WA powder exhibits needle-like and platelet-like structures.

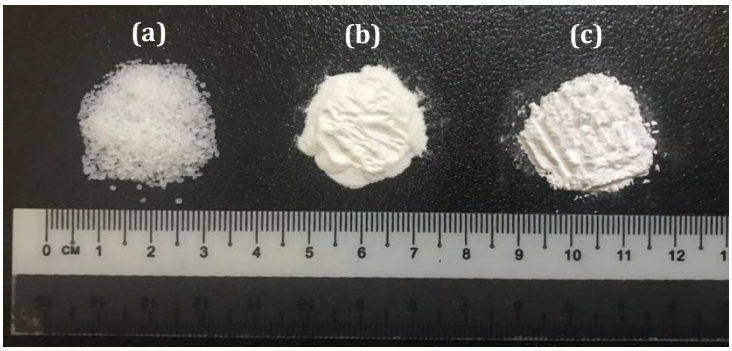

Fig. 1 *Raw materials (a) PLA coarse powder; (b) PA12 powder; (c) WA powder*

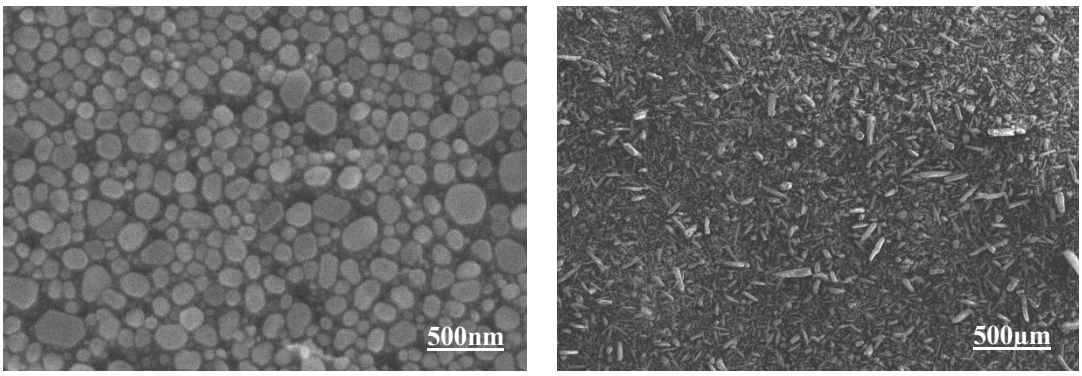

Fig. 2 *SEM images (a) PLA coarse powder; (b) WA powder*

2.2 Methodology

Material characterization was conducted for both the raw materials and the composite. The standard refractive indices (RI) of PLA (1.465), PA12 (1.52), and WA (1.63) were used as input parameters for the particle size distribution analysis using the Malvern Panalytical Mastersizer 2000. These RI values influence how the laser light is scattered as it passes through the samples, and are essential for accurate determination of particle size. Materials with different refractive indices interact with light differently, affecting the interpretation of scattering patterns. Thus, using the correct RI ensures the precision of particle size measurements.. Scanning Electron Microscopy (SEM) and Energy-Dispersive X-ray Spectroscopy (EDX) analyses were performed using a Hitachi SU3500 to study the morphological characteristics and elemental composition of the materials. Three composites consisting of 80PLA/20PA12 with the addition of 5, 10, and 15 wt.% of WA were prepared using an Internal Mixer Rheomix 600. The mixing process was conducted at a temperature of 185°C with a speed of 50 rpm, and the duration was approximately 50 minutes to ensure homogeneity and well-dispersed powders within the composites. Rheological analysis was carried out using a Bohlin Instrument RH2000 capillary rheometer, with a shear rate range of 20-1000 s^{-1} and temperatures of 140°C, 150°C, and 160°C. These temperatures were selected to stimulate the shear-flow behavior near the melting points of PLA and PA12 (150- 180 °C) and to mimic the pre-

printing extrusion behavior. The die used for this analysis had a diameter of 1 mm, in accordance with ASTM D3835 standard.

3. Results and Discussion

3.1 Particle Size Distribution

The particle size distribution analysis graph, depicted in Fig. 3 of the raw materials—PLA coarse powder, PA12, and WA powders—depicts unimodal distributions for each material, indicating a consistent and uniform particle size distribution within each sample. Table 1 provides the particle size distribution values (D10, D50, and D90) for each material. These values represent the particle sizes at which 10%, 50%, and 90% of the particles are smaller than that size, respectively. The PLA coarse powder exhibits the largest particle size, with a peak indicating the majority of particles are within the higher micrometer range, as confirmed by D10, D50, and D90 values of 486.142 µm, 847.884 µm, and 1450.521 µm, respectively. PA12 particles are smaller, showing a narrower distribution peak in the mid-micrometer range, with corresponding D10, D50, and D90 values of 37.998 µm, 59.271 µm, and 92.469 µm. WA powders demonstrate the smallest particle sizes with a peak in the lower micrometer range, reflected by D10, D50, and D90 values of 3.526 µm, 11.276 µm, and 35.988 µm.

The differences in particle sizes and specific surface areas among PLA (0.00775 m^2/g), PA12 (0.107 m^2/g), and WA (0.783 m^2/g) powders are critical for understanding their blending behaviour and interactions during composite formation. The large particles of PLA, combined with the smaller particles of PA12 and the fine particles of WA interact to influence the mixing behavior and dispersion and define the interfacial interactions within the composite. Similar behavior has been observed in composite blends where coarse and fine filler fractions and the strength of their interfaces significantly affect dispersion patterns, morphology, and mechanical performance (12). This, in turn, will affect the mechanical and rheological properties of the composite, which are crucial for its performance in FDM 3D printing applications.

The different peak of the unimodal distribution of raw materials suggests uniformity in particle sizes, which can contribute to a more homogeneous composite material. This different peak of uniformity can lead to consistent mechanical properties and performance of polymer-ceramic composite and lower polymerization shrinkage because the ceramic particles are uniformly distributed within the polymer matrix, thereby reducing voids within the matrix (13). Additionally, an unimodal distribution indicates that particles are not clustered (agglomerated) together, which could otherwise result in populations of two distinct sizes. Uniform particle size distribution can enhance consistent material flow during the feeding process, reduce extrusion defects, and improve packing density, potentially leading to denser filaments with improved mechanical properties.

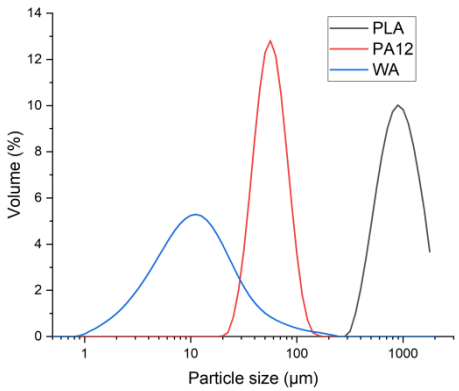

Fig. 3 *Particle size distribution curve of raw materials*

Table 1 *Particle size distribution analysis of raw materials*

Powder samples	Refractive Index (RI)	Specific surface area (m^2/g)	Particle Size Distribution (µm)		
			D10	D50	D90
PLA	1.465	0.00775	486.142	847.884	1450.521
PA12	1.520	0.107	37.998	59.271	92.469
WA	1.630	0.783	3.526	11.276	35.988

Int. Journal of Integrated Engineering Vol. 17 No. 5 (2025) p. 77-86

3.2 Morphological and Elemental Analyses

The SEM images in Fig. 4 illustrate the morphological changes in PLA/PA12 composites with the addition of 5, 10, and 15 wt.% WA ceramic particles. The SEM images indicate that the PLA/PA12 composite with 5 wt.% WA exhibits a relatively smooth surface, with some visible dispersion of the WA particles throughout the matrix. As the WA content increases, the composites exhibit a more pronounced sea-island morphology with distinct matrix droplets. In the 10 wt.% WA composites, noticeable white crystalline WA particles are dispersed within the matrix, showing a more prominent matrix-droplet morphology, suggesting good compatibility between the PLA/PA12 matrix and the WA ceramic particles at this concentration. The 15 wt.% WA composite prominently displays the sea-island morphology with distinct droplets, indicating higher WA particle dispersion. The sea-island morphology was formed due to the immiscibility of the PLA/PA12 blends (8).

Additionally, the surface morphology becomes rougher with increasing WA content, especially 15 wt.% WA composites showing a more significant presence of agglomerates on the surface compared to the 5 wt.% WA and 10 wt.% WA composites. The agglomeration of WA particles, which act as local strain concentrators in the PLA/PA12 matrix, will lead to poor interfacial interaction between the ceramic and polymer matrix (14,15). An increased amount of ceramic particles, resulting in more agglomeration, will adversely affect the mechanical strength of the composite (16).

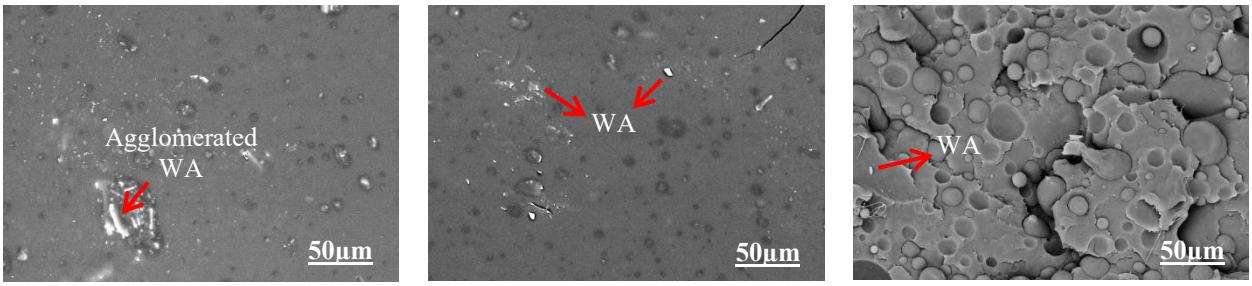

(a) **(b)** **(c)**

Fig. 4 *SEM images of PLA/PA12 composite with (a) 5 wt.% WA; (b) 10 wt.% WA; (c) 15 wt.% WA*

The EDX analysis, as shown in Fig. 5, corroborates the observations from SEM, revealing peaks corresponding to Carbon (C) and Oxygen (O), the primary constitutional elements of the polymers used in this study—namely PLA and PA12. These elements are consistent with the polymeric structure of both materials (11). All composite samples show clear evidence of the presence of wollastonite (WA) ceramic particles within the polymer matrix, as indicated by the expected peaks of Calcium (Ca) and Silicon (Si), which are characteristic of WA (17,18). The trace amounts of Ca and Si further demonstrate the incorporation of WA within the composite. In the 5 wt.% WA composite, weak peaks of Ca and Si suggest a relatively low concentration of WA, as evidenced by the lower weight percentages of Ca (2.1%) and Si (1.6%). This indicates that the ceramic filler is present but not in significant amounts. Conversely, the 10 wt.% WA composite displays more prominent peaks for Ca and Si, indicating a higher presence of WA particles in the polymer matrix. The weight percentages of Ca (6.7%) and Si (23.4%) in this composite confirm the increased incorporation of WA. Similarly, the 15 wt.% WA composite shows the strongest peaks for Ca and Si, reflecting the significant inclusion of WA. The weight percentages of Ca (18.3%) and Si (13.9%) are the highest among the samples, indicating the most substantial incorporation of the ceramic filler into the composite. The EDX analysis demonstrates a positive correlation between the increasing WA content and the corresponding rise in Ca and Si peaks. This confirms that the higher the WA content, the greater the presence of calcium and silicon-rich ceramic particles within the composite, as evidenced by the progressive increase in weight and atomic percentages of Ca and Si.

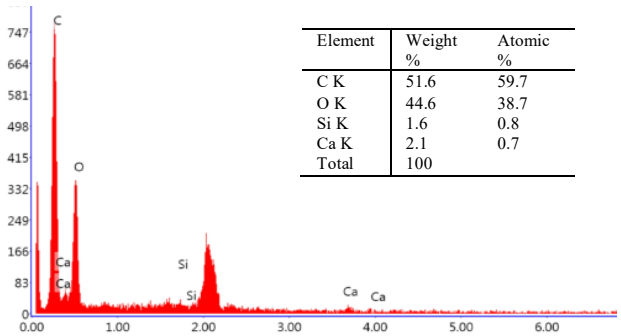

Element	Weight %	Atomic %
C K	51.6	59.7
O K	44.6	38.7
Si K	1.6	0.8
Ca K	2.1	0.7
Total	100	

(a)

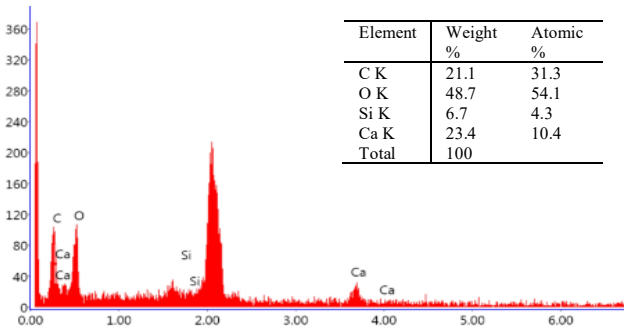

Element	Weight %	Atomic %
C K	21.1	31.3
O K	48.7	54.1
Si K	6.7	4.3
Ca K	23.4	10.4
Total	100	

(b)

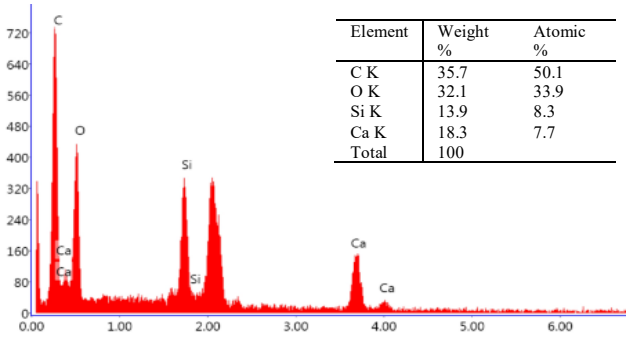

Element	Weight %	Atomic %
C K	35.7	50.1
O K	32.1	33.9
Si K	13.9	8.3
Ca K	18.3	7.7
Total	100	

(c)

Fig. 5 *EDX analysis of PLA/PA12 composite with (a) 5 wt.% WA; (b) 10 wt.% WA; (c) 15 wt.% WA. The spectra show elemental composition confirming increasing Ca and Si content with higher WA concentrations*

The combination of SEM images and EDX analysis provides valuable insights into the morphological and compositional changes in PLA/PA12 composites as the content of WA ceramic particles increases. These observations are crucial for understanding the structure-property relationships and potential applications of these composite materials. Increasing the WA content enhances the distribution of ceramic particles within the polymer matrix, contributing to the observed morphological changes. This uniform distribution is likely to impact the mechanical properties and performance of the composites, potentially leading to improved material characteristics suitable for FDM 3D printing applications. The rougher surface morphology and agglomerates at higher WA content suggest some level of incompatibility between the matrix and the filler particles, which could affect the mechanical properties of the composite.

3.3 Rheological Analysis

The rheological analysis of PLA/PA12 composites with varying concentrations of WA ceramic particles (5, 10, and 15 wt.%) at different temperatures (140°C, 150°C, and 160°C) is illustrated in Fig. 6. The graphs exhibit pseudoplastic behavior, characterized by a decrease in viscosity with increasing shear rate. This behavior is advantageous in 3D printing as it facilitates the smooth deposition of material during printing, preventing issues such as filament backflow, die swelling, buckling, and nozzle clogging (4). Pseudoplastic or shear-thinning behaviour is a non-Newtonian fluid behavior where the viscosity decreases with increasing shear rate. This characteristic is beneficial in 3D printing because it allows the material to flow easily through the nozzle under high shear rates and regain viscosity after deposition, thus maintaining the shape and stability of the printed structure (19). Comparing the viscosity ranges of all composites, it is evident that the addition of WA particles increases the viscosity, with the highest viscosity observed in the 15 wt.% WA composite. However, all composites exhibit a significant decrease in viscosity with increasing shear rate, consistent with pseudoplastic behavior ensuring good flowability (20).

For 3D printing applications, the ideal viscosity range typically falls between 10^2 and 10^5 Pa.s at the shear rates encountered during printing (21). For example, the PLA/PA12 composite with 5, 10, and 15 wt.% WA at 140°C exhibited viscosities of 8472 Pa.s, 5919 Pa.s, and 20710 Pa.s, respectively, which fall within this range, suggesting their suitability for 3D printing. However, the higher viscosity of the 15 wt.% WA composite at lower temperatures, where the range significantly deviates from those of the 5 wt.% WA and 10 wt.% WA composites, might pose challenges such as increased resistance to flow, potentially leading to issues like nozzle clogging. Generally, viscosity decreases with increasing temperature because higher temperatures enhance the mobility of polymer chains within the material, facilitating easier flow.

Int. Journal of Integrated Engineering Vol. 17 No. 5 (2025) p. 77-86

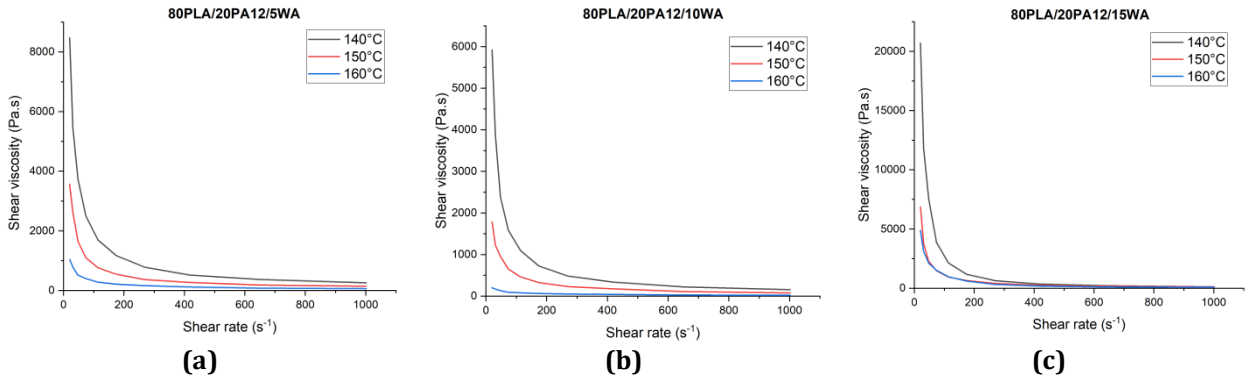

Fig. 6 *Rheological analysis of PLA/PA12 composite with (a) 5 wt.% WA; (b) 10 wt.% WA; (c) 15 wt.% WA*

The flow behavior index, *n* is crucial in rheological analysis as it indicates the type of flow behavior exhibited by the material. For pseudoplastic fluids, the *n* value typically falls between 0 and 1, reflecting a decrease in viscosity with increasing shear rate. This behavior is advantageous for 3D printing as it ensures smooth material deposition, reducing the risk of printing defects (22). The *n* value is derived from the Power-Law equation as stated in Equation (1), where η represents viscosity, Kstands for consistency, γ denotes shear rate, and *n* is the exponent representing the flow behaviour index. The *n* values for PLA/PA12 composites with varying concentrations of WA (5, 10, 15 wt.%) at different temperatures (140°C, 150°C, and 160°C) confirm this pseudoplastic behavior.

$$\eta = K\gamma^{n-1} \quad (1)$$

Based on the provided data in Table 2, all composites exhibit *n* values between 0 and 1, confirming their pseudoplastic nature. At 140°C, the composites exhibit the lowest *n* values (0.108 for 5 wt.% WA, 0.073 for 10 wt.% WA, and 0.123 for 15 wt.% WA), indicating higher viscosity at this temperature. This observation aligns with the rheological graphs in Fig. 6, where higher viscosities are noted at lower temperatures. Conversely, higher *n* values were observed at 150°C and 160°C, indicating lower viscosity at these higher temperatures. For example, at 160°C, the *n* values are 0.277 for 5 wt.% WA, 0.439 for 10 wt.% WA, and 0.283 for 15 wt.% WA. Notably, the 15 wt.% WA composite exhibits fluctuating *n* values, which could indicate inconsistencies in its flow behaviour at different temperatures. Specifically, the *n* value of 0.439 at 160°C for the 10 wt.% WA composite is within the optimal range, suggesting stable and desirable flow properties for 3D printing.

Table 2 *Flow behaviour index, n of all composites*

Composites	Temperature (ºC)	Flow behaviour index, *n*
PLA/PA12/5 wt.% WA	140	0.108
	150	0.162
	160	0.277
PLA/PA12/10 wt.% WA	140	0.073
	150	0.205
	160	0.439
PLA/PA12/15 wt.% WA	140	0.123
	150	0.312
	160	0.283

The rheological analysis graph and the flow behavior index, *n* for all PLA/PA12 composites with varying WA concentrations (5, 10, and 15 wt.%), the 10 wt.% WA composite emerges as the most optimal for 3D printing applications. It demonstrated that all composites exhibited pseudoplastic behavior, characterized by a decrease in viscosity with increasing shear rate, which is advantageous for smooth material deposition and minimizing printing defects. The *n* values for all composites fall within the range of 0 to 1, confirming their pseudoplastic nature. Notably, the 10 wt.% WA composite exhibited consistent *n* values across different temperatures, with an *n* value of 0.073 at 140°C, 0.297 at 150°C, and 0.439 at 160°C. This trend indicates that the 10 wt.% WA composite maintains a balanced pseudoplastic behaviour across the temperature spectrum, ensuring reliable flow characteristics. In contrast, the 5 wt.% WA and 15 wt.% WA composites showed more variability in their flow

behaviour, with the 15 wt.% WA composite, in particular, exhibiting fluctuating *n* values. Therefore, considering the consistent pseudoplastic behavior observed, the PLA/PA12/10 wt.% WA composite is deemed optimal for 3D printing applications with constant *n* value and lower viscosity which support better layer adhesion and dimensional stability during FDM printing.

3.4 Physical Observation of Extruded Composite Material

Based on Fig. 7 of the extruded materials of PLA/PA12 composites with varying concentrations of WA (5 wt.% WA, 10 wt.% WA, and 15 wt.% WA) from rheological analysis, several key insights can be derived. The extruded composite with 5 wt.% WA exhibits a rough surface with inconsistencies in its circular cross-section, indicating an uneven flow and potential issues with the uniformity of the material during the extrusion process. Similarly, the 15 wt.% WA composite displays the roughest surface among the three, with visible clusters of ceramic particles embedded, further suggesting significant challenges in achieving a smooth and consistent extrudate (17). In contrast, the 10 wt.% WA composite demonstrates the most promising characteristics: a smooth surface, consistent diameter, and persistent circular cross-section, indicating a more stable and controlled flow during extrusion. Moreover, a higher concentration of ceramic particles causes the colour to become yellowish (10).

The rougher surfaces observed in the 5 wt.% WA and 15 wt.% WA composites can be attributed to the imbalance in the distribution and interaction of WA particles within the PLA/PA12 matrix. For the 5 wt.% WA composite, the lower concentration of WA particles may lead to insufficient reinforcement, causing irregular flow patterns and surface roughness as illustrated in Fig. 7 (a). On the other hand, the 15 wt.% WA composite's high concentration of ceramic particles likely results in agglomeration, leading to increased resistance to flow, which manifests as surface roughness and inconsistencies (23,24). The 10 wt.% WA composite, however, strikes an optimal balance in the distribution of WA particles within the matrix. This balance minimizes agglomeration while providing adequate reinforcement, resulting in a smooth and consistent extrudate.

These physical observations are crucial as they directly impact the next steps in the 3D printing process, including filament fabrication and deposition. A smooth and consistent extrudate ensures uniform filament quality, essential for precise and reliable 3D printing. It also reduces the likelihood of nozzle clogging and other printing defects, thereby enhancing the overall performance and reliability of the 3D-printed structures. The superior quality of the 10 wt.% WA extruded composite can be attributed to its optimal rheological properties. The balance of WA concentration likely provides the right viscosity and flow behaviour, allowing for smooth and consistent extrusion.

Based on this analysis, the 10 wt.% WA composite emerges as the best-performing material for subsequent processing and 3D printing applications due to its superior flow characteristics and physical consistency. The smooth and consistent nature of the 10 wt.% WA extruded composite suggests it would be ideal for producing high-quality filaments with uniform diameter and surface finish. This consistency is crucial for ensuring reliable feeding through the 3D printer nozzle and achieving precise layer deposition. Conversely, the rougher surfaces and inconsistent profiles of the 5 wt.% WA and 15 wt.% WA composites could lead to filament production and 3D printing challenges. Irregular filaments may cause inconsistent extrusion rates, potential nozzle clogs, and variations in layer thickness during printing, all of which can compromise the quality and structural integrity of the printed parts.

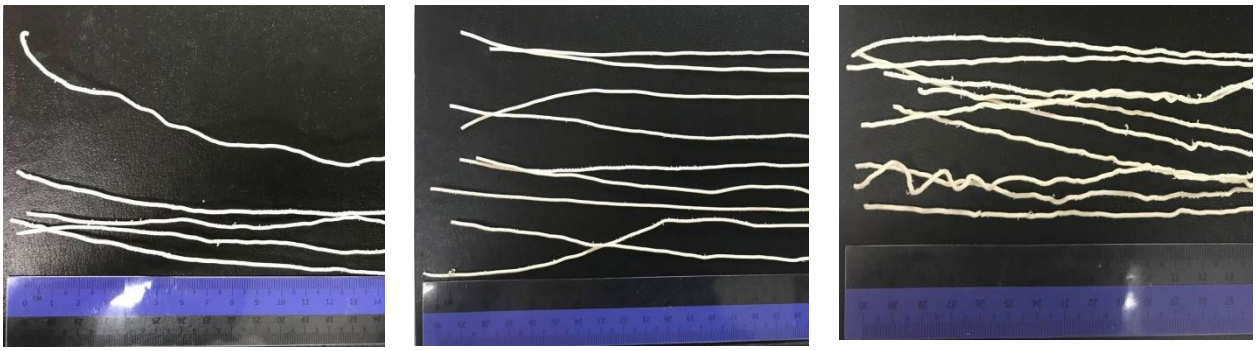

(a) **(b)** **(c)**

Fig. 7 *Extruded material of PLA/PA12 composite with (a) 5 wt.% WA; (b) 10 wt.% WA; (c) 15 wt.% WA*

4. Conclusion

A comprehensive analysis was conducted on the material characterization and rheological properties of PLA/PA12 composites with different concentrations of WA (5%, 10%, and 15%). SEM analysis revealed a more uniform morphology in the 10 wt.% WA composite, with well-dispersed WA particles, compared to the

agglomeration observed in the 15 wt.% WA composite and the insufficient particle distribution in the 5 wt.% WA composite. The consistent *n* values across different temperatures of 10 wt.% WA composite, 0.073, 0.297, and 0.439 indicated a pseudoplastic behavior optimal for 3D printing applications, providing a balance between viscosity and flow. Additionally, the extruded material of the 10 wt.% WA composite exhibited a smooth surface, consistent diameter, and a persistent circular cross-section, which are crucial for high-quality filament fabrication and reliable 3D printing. In contrast, the 5 wt.% WA and 15 wt.% WA composites showed rougher surfaces and inconsistencies attributed to insufficient or excessive WA content, respectively. Overall, the integration of rheological and material characterization analyses underscores the 10 wt.% WA composite's balanced composition and optimal performance, making it the most promising candidate for efficient and effective 3D printing processes. This composite's superior material properties and rheological behaviour ensure high-quality filament production and consistent 3D printed structures. Nonetheless, the mechanical testing of this composite and actual 3D printing assessment need to be explored in future research.

Acknowledgement

The authors would like to thank Universiti Teknologi MARA (UiTM) for the financial support under the Geran Insentif Penyeliaan (Project File No. RD/47/002/2025), and UiTM Shah Alam for providing laboratory facilities and technical support throughout this research.

Conflict of Interest

The authors declare no conflict of interest regarding the publication of this research study.

Author Contribution

The authors contributed equally to both original draft preparation and review and editing of this manuscript.

References

[1] Melo P, Ferreira AM, Waldron K, Swift T, Gentile P, Magallanes M, Marshall M, Dalgarno K. Osteoinduction of 3D printed particulate and short-fibre reinforced composites produced using PLLA and apatite-wollastonite. Composites Science and Technology. 2019 Nov 10;184:107834, https://doi.org/10.1016/j.compscitech.2019.107834

[2] Haq RHA, Taib I, Rahman MNA, Haw HF, Abdullah H, Ahmad S, et al. Mechanical properties of PCL/PLA Composite sample produced from 3D printer and injection molding. International Journal of Integrated Engineering. 2019;11(5):102–8, https://doi.org/10.30880/IJIE.2019.11.05.014

[3] Moreno AI, Orozco Y, Ocampo S, Malagón S, Ossa A, Peláez-Vargas A, et al. Effects of Propolis Impregnation on Polylactic Acid (PLA) Scaffolds Loaded with Wollastonite Particles against Staphylococcus aureus, Staphylococcus epidermidis, and Their Coculture for Potential Medical Devices. Polymers (Basel). 2023 Jun 1;15(12), https://doi.org/10.3390/polym15122629

[4] Calafel I, Aguirresarobe RH, Peñas MI, Santamaria A, Tierno M, Conde JI, et al. Searching for Rheological Conditions for FFF 3D Printing with PVC Based Flexible Compounds. Materials 2020, Vol 13, Page 178 [Internet]. 2020 Jan 1 [cited 2025 Jun 13];13(1):178, https://doi.org/10.3390/MA13010178

[5] Anderegg DA, Bryant HA, Ruffin DC, Skrip SM, Fallon JJ, Gilmer EL, et al. In-situ monitoring of polymer flow temperature and pressure in extrusion based additive manufacturing. Addit Manuf. 2019 Mar 1;26:76–83, https://doi.org/10.1016/j.addma.2019.01.002

[6] Raj A, Prashantha K, Samuel C. Compatibility in biobased poly(L-lactide)/polyamide binary blends: From melt-state interfacial tensions to (thermo)mechanical properties. J Appl Polym Sci. 2020 Mar 10;137(10), https://doi.org/10.1002/app.48440

[7] Raj A, Samuel C, Prashantha K. Role of Compatibilizer in Improving the Properties of PLA/PA12 Blends. Front Mater. 2020 Jul 17;7, https://doi.org/10.3389/fmats.2020.00193

[8] Murariu M, Arzoumanian T, Paint Y, Murariu O, Raquez JM, Dubois P. Engineered polylactide (PLA)–polyamide (PA) blends for durable applications: 1. PLA with high crystallization ability to tune up the properties of PLA/PA12 blends. European Journal of Materials. 2023;3(1):1–36, https://doi.org/10.1080/26889277.2022.2113986

[9] Choudhary R, Bulygina I, Lvov V, Zimina A, Zhirnov S, Kolesnikov E, et al. Mechanical, Structural, and Biological Characteristics of Polylactide/Wollastonite 3D Printed Scaffolds. Polymers (Basel). 2022 Oct 1;14(19), https://doi.org/10.3390/polym14193932

[10] Lin YH, Chiu YC, Shen YF, Wu YHA, Shie MY. Bioactive calcium silicate/poly-ε-caprolactone composite scaffolds 3D printed under mild conditions for bone tissue engineering. J Mater Sci Mater Med. 2018 Jan 1;29(1), https://doi.org/10.1007/s10856-017-6020-6

[11] Ramos-Rodriguez DH, Pashneh-Tala S, Bains AK, Moorehead RD, Kassos N, Kelly AL, et al. Demonstrating the Potential of Using Bio-Based Sustainable Polyester Blends for Bone Tissue Engineering Applications. Bioengineering. 2022 Apr 1;9(4), https://doi.org/10.3390/bioengineering9040163

[12] Nasrin T, Adisa AO, Hansen CJ, Pourkamali-Anaraki F, Jensen RE, Peterson AM. Emergent mechanical properties in highly filled additively manufactured polymer composites. MRS Communications. 2024 Aug;14(4):503-10, https://doi.org/10.1557/s43579-024-00530-x

[13] Wang R, Habib E, Zhu XX. Evaluation of the filler packing structures in dental resin composites: From theory to practice. Dental Materials. 2018 Jul 1;34(7):1014-23, https://doi.org/10.1016/j.dental.2018.03.022

[14] Wu D, Spanou A, Diez-Escudero A, Persson C. 3D-printed PLA/HA composite structures as synthetic trabecular bone: A feasibility study using fused deposition modeling. J Mech Behav Biomed Mater. 2020 Mar 1;103, https://doi.org/10.1016/j.jmbbm.2019.103608

[15] Pandele AM, Constantinescu A, Radu IC, Miculescu F, Voicu SI, Ciocan LT. Synthesis and characterization of PLA-micro-structured hydroxyapatite composite films. Materials. 2020 Jan 1;13(2), https://doi.org/10.3390/ma13020274

[16] Olam M, Tosun N. 3D-printed polylactide/hydroxyapatite/titania composite filaments. Mater Chem Phys. 2022 Jan 15;276, https://doi.org/10.3390/ma13020274

[17] Diez-Escudero A, Andersson B, Persson C, Hailer NP. Hexagonal pore geometry and the presence of hydroxyapatite enhance deposition of mineralized bone matrix on additively manufactured polylactic acid scaffolds. Materials Science and Engineering C. 2021 Jun 1;125, https://doi.org/10.1016/j.msec.2021.112091

[18] Gandolfi MG, Zamparini F, Degli Esposti M, Chiellini F, Aparicio C, Fava F, et al. Polylactic acid-based porous scaffolds doped with calcium silicate and dicalcium phosphate dihydrate designed for biomedical application. Materials Science and Engineering C. 2018 Jan 1;82:163–81, https://doi.org/10.1016/J.ADDMA.2021.101944

[19] Bertolino M, Battegazzore D, Arrigo R, Frache A. Designing 3D printable polypropylene: material and process optimisation through rheology, Addit. Manuf. 40 (2021) 101944 [Internet]. 2021, https://doi.org/10.1016/j.addma.2021.101944Get rights and content

[20] Amin MM, Adelin NS, Sulong AB, Muhamad N. Rheological Analysis of Zirconia-Hydroxyapatite with Bi-Modal System of Binders; Low-Density Polyethylene and Palm Stearin. International Journal of Integrated Engineering. 2023 Oct 19;15(5):179-88, https://doi.org/10.30880/ijie.2023.15.05.019

[21] Bragaglia M, Lamastra FR, Russo P, Vitiello L, Rinaldi M, Fabbrocino F, et al. A comparison of thermally conductive polyamide 6-boron nitride composites produced via additive layer manufacturing and compression molding. Polym Compos. 2021 Jun 1;42(6):2751–65, https://doi.org/10.1002/pc.26010

[22] Naranjo JA, Berges C, Campana R, Herranz G. Rheological and mechanical assessment for formulating hybrid feedstock to be used in MIM & FFF. Results in Engineering. 2023 Sep 1;19, https://doi.org/10.1016/j.rineng.2023.101258

[23] Wang W, Zhang B, Li M, Li J, Zhang C, Han Y, et al. 3D printing of PLA/n-HA composite scaffolds with customized mechanical properties and biological functions for bone tissue engineering. Compos B Eng. 2021 Nov 1;224, https://doi.org/10.1016/j.compositesb.2021.109192

[24] Bakhshi R, Mohammadi-Zerankeshi M, Mehrabi-Dehdezi M, Alizadeh R, Labbaf S, Abachi P. Additive manufacturing of PLA-Mg composite scaffolds for hard tissue engineering applications. J Mech Behav Biomed Mater. 2023 Feb 1;138, https://doi.org/10.1016/j.jmbbm.2023.105655